EFFECT OF WETTABILITY ON NUCLEATE BOILING

Valente T., Teodori E., Moita A.S. * and Moreira A.L.N.
*Author for correspondence
IN + - Department of Mechanical Engineering,
Instituto Superior Técnico, Universidade de Lisboa,
Av. Rovisco Pais, 1, 1049-001 Lisbon,
Portugal,
E-mail: anamoita@dem.ist.utl.pt

ABSTRACT

Heat transfer enhancement at liquid-solid interfaces is often achieved by modifying the surface properties. However, deep efforts to describe the actual role of surface modification only started at the 1980's and much work has left undone since then. The wettability is a key parameter governing heat, mass and momentum transport at liquid-solid interfaces. However it is usually quantified using macroscopic quantities, which cannot be related with the micro-and-nano-scale phenomena occurring at the interface. In this context, the present paper revises the potential and limitations of using macroscopic apparent contact angles to predict the wetting regimes. Then, these angles are used to relate the wetting regimes with bubble dynamics and heat transfer processes occurring at pool boiling. The results show that the macroscopic angles are useful to establish general trends and differentiate bubble dynamics behaviour occurring for opposite wetting regimes. However, milder wetting changes occurring within each regime, caused, for instance, by surface topography are not well captured by the apparent angle, as the surface topography is not scaled to affect this macroscopic angle, although it can clearly influence the bubble formation and departure mechanisms and, consequently the heat transfer coefficients. In line with this, the concept of the micro-scale contact angle, as introduced by Phan et al. [1] is used here together with a geometrical parameter to include the effect of surface topography, to describe the role of the wettability on bubble dynamics. Based on this analysis, a multi-scale approach is proposed to include the role of wettability on correlations predicting the pool boiling heat transfer coefficients.

INTRODUCTION

Changing surface properties has been addressed for many years to improve heat transfer at liquid-solid interfaces, namely in pool boiling heat transfer. The fast development of micro-and-nano-fabrication techniques offered to the researchers the opportunity to quickly experiment a variety of scales and shapes. So, from the pioneering work of Corty and Foust [2] in which the surfaces were micro-patterned with structures of hundreds of microns in size, surface treatment methods swiftly evolved to nanocoatings (*e.g.* [3-4]), suddenly decreasing the scale. The search for good performances, often associated to the
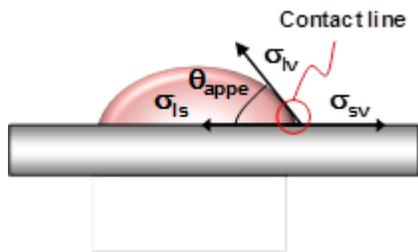
NOMENCLATURE

a	[μm]	Length of the side of the square micro-cavities in the micro-patterned surfaces
A	[cm^2]	Heated area of the surface
A_i	[mm^{-2}]	Interfacial area
C_p	[Jkg^{-1}K^{-1}]	Specific heat
D_b	[mm]	Bubble departure diameter
f_b	[Hz]	Bubble emission frequency
f_r	[-]	Fraction of solid wetted by the liquid
g	[ms^{-2}]	Acceleration of gravity
h	[Wcm^{-2}K]	Heat transfer coefficient
h_{fg}	[kJ/kg]	Latent heat of evaporation
h_R	[μm]	Depth of the square micro-cavities in the micro-patterned surfaces
k	[Wm^{-1}K^{-1}]	Thermal conductivity
Lc	[mm]	Characteristic length (capillary length)
NSD	[m]	Nucleation sites density
q''	[Wcm^{-2}]	Heat flux
R_a	[μm]	Surface mean roughness
r_f	[-]	Roughness factor
R_z	[μm]	Surface peak-to-valley roughness
S	[μm]	Distance between the micro-cavities in the micro-patterned surfaces
T	[K]	Temperature
t_{wn}	[s]	Waiting time

Greek symbols

α	[m^{2}s^{-1}]	Thermal diffusivity
λ	[μm]	Fundamental wavelength of the roughness profile
μ	[Nsm^{-2}]	Dynamics viscosity
θ_{appd}	[º]	Apparent dynamic contact angle
θ_{appe}	[º]	Apparent equilibrium contact angle
θ_{appqs}	[º]	Apparent quasi-static contact angle
θ_{ms}	[º]	Micro-scale contact angle
ρ	[kgm^{-3}]	Density
σ	[N.m^1]	Interfacial tension

Subscripts

b	Bubble
ev	Evaporation
l	Liquid
nc	Natural convection
q	Quenching
s	Solid
sat	Saturation
tot	Total
v	Vapor
W	Wall

maximization of the heat fluxes provided or removed, for liquid heating or cooling applications has based the experimental procedure in a trial-and-error approach, given the variety of surface treatments easily available. However, as recently pointed by Cheng et al. [5], the deep efforts to describe the actual processes governing the effect of surface modification on the energy, mass and momentum transport at interfaces only started at the 1980's and much work has left undone since then. Also, the surface treatment is often multi-scaled, but the description of the governing phenomena is not following this fast scaling down of the surface structuring and modification. As reviewed by Moreira [6], the main processes governing heat transfer at liquid-solid interfaces must be considered within a multi-scale perspective and in this context, several quantities must be well identified, or their effect will be misinterpreted. For instance, a multi-scale approach to describe and control the hydrodynamics, heat transfer and phase change in droplets and films has been recently proposed by Gambaryan-Roisman [7], which relates surface modification with wettability. Indeed wettability is a key factor controlling interfacial phenomena, as it quantifies how well a liquid spreads over the surface. The spreading mainly depends on the balance between adhesive and cohesive intermolecular forces, thus being a micro or even nano-scale governed process, but is often quantified based on the macroscopic thermodynamic balance between the interfacial tensions at liquid-solid-vapor interfaces. Hence, the wettability is often quantified by the apparent contact angle θ_{appe}, which is obtained at the equilibrium between the interfacial tensions acting as a droplet is gently deposited over the surface (Figure 1). This balance of interfacial tensions is given by the well-known Young equation [8]:

$$\sigma_{lv}\cos \theta_{appe} + \sigma_{ls} = \sigma_{sv} \qquad (1)$$

Here σ stands for the interfacial tension between liquid (l), solid (s) and vapor (v) phases that meet at the contact line.

Figure 1 Definition of the equilibrium apparent angle, based on the balance between the interfacial tensions.

Based on this angle, it is widely accepted that a surface is lyophilic (i.e. promotes the liquid spreading) for $0 < \theta_{appe} < 90^\circ$ and lyophobic (i.e. repels the liquid) for $\theta_{appe} > 90^\circ$. The terms hydrophilic/hydrophobic, which are commonly used for liquid attractive/repellent surfaces derive from the specific attraction/repellency of water, so that generally the surfaces are lyophilic or lyophobic. Complete wetting/no wetting situations are ideally given by $\theta_{appe} = 0^\circ$ and $\theta_{appe} = 180^\circ$, respectively, but in practice, many authors consider that a surface is superhydrophilic for $\theta_{appe} < 10^\circ$, hydrophilic for $0 < \theta_{appe} < 90^\circ$,

hydrophobic for $90^\circ < \theta_{appe} < 150^\circ$ and superhydrophobic for $\theta_{appe} > 150^\circ$.

Eq. (1) is basically obtained in equilibrium conditions, by the minimization of the Gibbs energy of the system formed by the surface, the droplet and the surrounding vapor. For a determined temperature and pressure and for a uniform chemical composition of the surface, this equation can be written generically as:

$$G = \sigma_{lv}A_{ilv} + \sigma_{ls}A_{ils} + \sigma_{sv}A_{isv} \qquad (2)$$

where A_i is the interfacial area.

From the macroscopic point of view, the surface topography will alter this equilibrium equation, as it affects the interfacial area, so that Young equation is not valid for rough surfaces. Instead, a roughness factor must be considered to correct the apparent angle. For the so-called homogeneous wetting regime, the liquid will wet completely the surface, thus penetrating within the roughness grooves. In this case, the Young balance is corrected as the Wenzel equation [9]:

$$\cos\theta_{appeWenzel} = r_f \cos\theta_{appe} \qquad (3)$$

where r_f is the roughness factor, which represents the ratio between the true to the apparent wetted area. If the liquid does not penetrate completely within the rough grooves, the corrected apparent contact angle is given by the Cassie and Baxter equation [10]:

$$\theta_{appeCassie-Baxter} = r_f \cos\theta_{appe} - f_r(r_f \cos\theta_{appe} + 1) \qquad (4)$$

where f_r is the projected area of the solid that is wetted by the liquid. This is the so-called heterogeneous wetting regime. The applicability of these equations is still a hot topic for discussion, (e.g. Marmur [11]), as they are macroscopically good approximations to estimate the contact angle, but do not address the phenomena occurring at the contact line, which mainly govern the spreading (e.g. [12]). This issue is usually solved by establishing the criteria leading to a metastable wetting regime, for which the energy of the tertiary system droplet-surface-vapor is minimized. Hence, a heterogeneous wetting regime may not be stable and may become homogeneous as long as an activation energy barrier is transposed and the contact line slowly moves (e.g. [13]). The apparent contact angles defined immediately before the advancing or receding motion of the contact line are quasi-static advance or receding (apparent) contact angles. The difference between the quasi-static advancing and receding contact angles is he hysteresis and is related to the irreversibility (energy dissipation at the contact line) which occurs as the contact line moves. These angles are still macroscopic and should not be confused with the dynamic advancing and receding contact angles, which are formed during a truly dynamic process in which the velocity of the contact line is not negligible [11].

In line with this, finding a universal criterion establishing the boundary of wetting regimes based on the apparent contact angles is not possible until they can be well related to the basic equilibrium of the adhesive and cohesive forces acting at the contact line, within a microscopic or eventually molecular scale [6]. So, a solution should be found within a multi-scale approach that can relate the macroscopic apparent angle to the actual governing processes occurring at the contact line within a micro-to-nano scale. This is a vital issue, as many

applications require a quantifiable macroscopic measure of the wettability, which in fact will affect governing processes that actually occur within the microscopic scale.
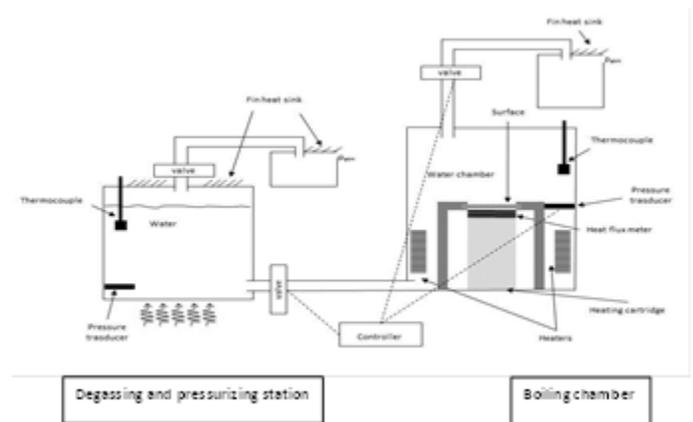
In the particular case of pool boiling applications, surface enhancement to improve pool boiling heat transfer is usually achieved by altering the surface topography and/or its chemistry. Both methods will affect the wettability, from the microscopic point of view, but they may not affect dramatically the value of the apparent contact angle. In many studies, both chemistry and topography are changed in a non-systematic way, so that it is difficult to quantify the actual role of each treatment, thus leading to misinterpretations on the values of the contact angle, which in turn are not well related to the observed phenomena. This is particularly important when dealing with nucleation. It is known that pool boiling heat transfer enhancement made by roughening the surface is based on the premise that it will increase the number of potential nucleation sites and will increase the wetted area, thus globally contributing to increase the heat transfer coefficients. However, the surface topography may not be sufficient to macroscopically act on the apparent contact angle, but can be significantly altering the bubble growth and several dynamic processes (e.g. interaction mechanisms). On the other hand, the chemical modification may be creating local heterogeneities, which may affect the critical availability function and free energy change, which are required to activate a nucleation site [5]. Hence, the global enhanced performance of hydrophilic surfaces with hydrophobic isles or biphilic surfaces, as experimentally proven by [14,15] seems to be related to a global increase of the active nucleation sites, that according to Cheng et al. [5] is often associated to rough boundaries imposed by the manufacturing process and not to the chemical modification. However, within micro or nanometric roughness amplitudes, a similar activation process can be achieved by a chemical imposed inhomogeneity. This issue has been recently raised by Bourdon et al. [16-17], but their studies were limited to stochastic roughness profiles and to very smooth surfaces.

In line with this, the present work suggests a first step within a multi-scale approach to relate the macroscopic apparent contact angle with the microscopic description of wettability and its effect on the nucleation and bubble dynamics and consequently on the heat transfer phenomena.

To cope with this, the apparent contact angle is dramatically changed to opposite wetting scenarios, in which the surface structuring is scaled differently. The scaling of the topography is then related to the apparent angle and the nucleation processes are discussed within these extreme wetting macroscopic scenarios. Then, mild wettability modification (obtained by surface structuring) is approached from a microscopic point of view and trends are settled to relate the apparent contact angle with the local angles associated to bubble formation. The heat transfer mechanisms can be further discussed, considering the role of nucleation and bubble dynamics. Based on this analysis, general trends are finally suggested to include this multi-scale approach in the relations predicting pool boiling heat transfer coefficients.

EXPERIMENTAL APPARATUS

Figure 2 presents a schematic view of the set-up.

Figure 2 Schematic representation of experimental apparatus.

The set-up is mainly composed by a degassing station in which the fluid is degassed, pressurized and constantly heated, a boiling chamber, in which the experiments are performed and a filling and evacuating circuit that connects the boiling chamber respectively to the degassing station and to the waste fluid container, being the later at ambient pressure. The pressure and the saturation temperature inside the boiling chamber are controlled. The entire heating section of the pool boiling test section is isolated with Teflon, from outside and the pool boiling chamber is isolated with rubber. Heaters disposed inside and on the outer surfaces of the boiling chamber are controlled by a PID controller to assure that the liquid remains inside the chamber at saturation temperature. The pressure is controlled by means of two electronic valves that respond to the measures given by a pressure transducer (OMEGA DYNE Inc) inside the pool, using a home-made software based loop control. This control system reacts to pressure variations in the order of 5mbar. The refilling and the entire measurement processes are automatically controlled by this software.

The temperatures are sampled using type K thermocouples. The signal is acquired and amplified with a National Instruments DAQ board plus a BNC2120. The acquisition frequency is 100Hz and the temperature is monitored for 20 seconds after reaching a stable condition (constant temperature variation which does not exceed $\pm0.5°C$).

MEASUREMENT PROCEDURES AND DIAGNOSTIC TECHNIQUES

The test surfaces are characterized in terms of topography and wettability, as described in the following paragraph. Then, pool boiling curves are constructed for each test surface, for pool boiling of various liquids. To infer on the possible effect of surface ageing during pool boiling experiments, the wettability, quantified by the apparent equilibrium contact

angle is verified after each boiling curve reconstruction. This procedure ensures the exact definition of the boundary conditions related to the wettability (one of the main parameters in study here) and allows inferring the effect of surface ageing on the wettability and, consequently on the pool boiling curves.

As the boiling curves are obtained, bubble dynamics and nucleation mechanisms are also characterized based on high speed visualization, using a high-speed camera (Phantom v4.2 from Vision Research Inc., with 512x512pixels@2200fps). Quantitative information regarding the bubble formation and departure (bubble dynamics, departure frequency, nucleation sites density, among others) are obtained from image post-processing procedures.

As for the working fluids, the present work considers the use of the dielectric fluid HFE 7000, ethanol and water. These fluids were selected since they can cover a wide range of the values of surface tension and of the relevant thermal properties such as the thermal conductivity, the heat capacity and the latent heat of evaporation, as shown in Table 1.

Table 1 Thermophysical properties of the liquids used in the present study, taken at saturation, at 1.013×10^5 Pa.

Property	Water	Ethanol	HFE7000
T_{sat} (°C)	100	78.4	34
ρ_l (kg/m^3)	957.8	736.4	1374.7
ρ_v (kg/m^3)	0.5956	1.647	4.01
μ_l (mN m/s^2)	0.279	0.448	0.3437
c_{pl} (J/kgK)	4217	3185	1352.5
k_l (W/mK)	0.68	0.165	0.07
h_{fg} (kJ/kg)	2257	849.9	142
σ_{lv} (N/m)x10^3	58	17	12.4

Preparation and characterization of the surfaces

The surfaces are prepared to have different topographical and chemical characteristics, to allow a systematic study of each parameter.

In terms of topography, the surfaces are prepared to have regular micro-patterns and stochastic roughness profiles. The surfaces with regular micro-patterns are custom made from silicon wafers, which are coated with aluminum (to allow a deeper etching) and afterwards with photoresist. The regular patterns are transferred by high resolution printing and photolithography and are then submitted to plasma etching for 5-7hours. Finally, wet etching is used to remove the aluminum coating. The surfaces are micro-structured with regular arrays of squared cavities, with fixed size length a=52µm and fixed depth h_R=20µm. The distance between the centers of the cavities, S is mainly the only variable distance, ranging between 300µm<S<1200µm. Surfaces with stochastic profiles are grafted and/or coated with a fluoropolymer based coating. For the surfaces displaying regular micro-patterns, the characteristic dimensions of a, h_R and S can be taken from roughness profiles, which are measured using a Dektak 3 profile meter (Veeco) with a vertical resolution of 200Angstroms. For the surfaces with stochastic profiles, these profiles are further processed to obtain the mean roughness (determined according to standard BS1134) and the mean peak-to-valley roughness (determined

following standard DIN4768), as performed in previous work (e.g. [18-19]).

Wettability was quantified by the equilibrium contact angle θ and by hysteresis, using an optical tensiometer THETA from Attension, The measurements are performed at room temperature (20ºC), using the pendant drop method. The angles are evaluated from the images taken within the tensiometer, using the camera adapted to a microscope. The images (with resolution of 15.6 µm/pixel, for the optical configuration used) are post-processed by a drop detection algorithm based on Young-Laplace equation (One Attension software). The accuracy of these algorithms is argued to be of the order of ± 0.1º [20].

Table 2 depicts the main topographical characteristics of the surfaces used in this study, together with the apparent equilibrium contact angles obtained with water, at room temperature. The values of the equilibrium angle are averaged from up to 15 measurements taken along different regions of the surface, to have a representative measure. Detailed procedure is described in [18]. Hysteresis is much higher than 10º for all the surfaces, except for surface S2, for which hysteresis is inferred to be around 8º. Although, as referred in the introduction, the definition of the exact boundaries between the various wetting regimes is still a hot topic for discussion, it is widely accepted that hydrophobic surfaces exhibit an equilibrium angle larger than 90º, while for superhydrophobic surfaces the contact angle should be higher than 150º. Given the relation between a possible irreversible motion of the contact line and the hysteresis, which could lead to a change in the wetting regime, the superhydrophobic surfaces should depict a hysteresis lower than 10º (e.g. [21]). In line with this, all the surfaces are hydrophilic or partially hydrophobic, exception made to surface S2, which is superhydrophobic.

All the surfaces are lyophilic in contact with ethanol and with HFE 7000.

Table 2 Main topographical and wetting characteristics of the surfaces.

	Ref.	a	h_R	S	R_a	R_z	θ
		[µm]	[µm]	[µm]	[µm]	[µm	[º]
Si	Smooth	≈ 0	≈ 0	≈ 0	-	-	86.0
Wafer							
	C1	52	20	304	-	-	90.0
	C2	52	20	400	-	-	91.5
	C3	52	20	464	-	-	71.5
	C4	52	20	626	-	-	86.5
	C5	52	20	700	-	-	95.0
	C6	52	20	800	-	-	60.5
	C7	52	20	1200	-	-	66.3
Alumin	S1				1..3	14.5	88

um					
Grafted Alumin um	S2		4	8	165

Pool boiling curves

The boiling curves are presented for each liquid and each heating surface by varying the imposed heat flux in steps of 1-5W/cm^2. Each curve is averaged from 3 experiments considering both heat flux increasing and decreasing (to infer on hysteresis effects). Exception is made when the ageing of the surface treatment would lead to change the wettability, after one boiling test. In this case, a series of curves was obtained, as a function of the contact angle, measured at the end of each test. The main uncertainties of the quantities related to the heat transfer are measurements are ±22.5%. The uncertainty for the temperature measurements is ±1.2% and is assessed following the procedures recommended in [22]. Detailed description of the measurement procedures and determination of error sources can be found in can be found in Moita et al. [23].

Image post-processing for the characterization of the nucleation mechanisms and bubble dynamics

The characterization of the nucleation mechanisms and bubble dynamics is based on the measurement of several quantities such as the departure diameter, the departure frequency, among others, which are obtained from high-speed visualization and image post-processing. The images are recorded with a frame rate of 2200fps. For the optical configuration used here, the spatial resolution is 9.346μm/pixel.

The bubble departure diameter is measured for each test condition from 300 to 1060 frames. For each image a mean value is averaged from 5-16 measurements for every nucleation site that is identified in the frame.

The accuracy of the measurements of the bubble departure diameter is ±9.346μm. Coalescence effects are confirmed based on visual inspection of the processed images.

The bubble departure frequency is estimated by determining the time elapsed between apparent departure events, which are counted for a defined time interval. The departure frequency is assessed, for each test condition, for at least five nucleation sites, which are evaluated based on extensive image post-processing of 300 to 1060 frames. The final value of the bubble departure frequency is the average between the frequencies of each nucleation site. The uncertainty associated to these measurements is ±1 fps.

Finally, the evaluation of the active nucleation sites density is evaluated for, at least ten frames, at different times during the single experiment. The final values of the active nucleation site density are an average of the ten evaluated values identified within the same region of interest. Detailed description of the measurement procedures is also presented in Moita et al. [23].

RESULTS AND DISCUSSION

Establishing the wetting regimes: the scale effect of surface topography
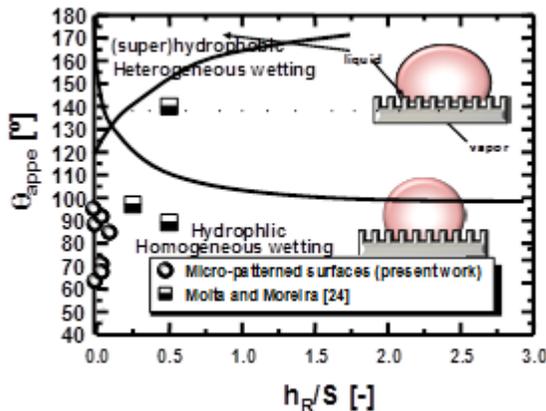
As briefly mentioned in the introduction, there is a wide discussion on the criteria to establish the boundary conditions between wetting regimes, based on apparent contact angle measurements. Most of the criteria are still grounded on the Wenzel and Cassie and Baxter equations (eqs. 3 and 4) being the key parameter the roughness pattern that will allow the surface tension forces to balance the Bernoulli pressure. Regular patterns are often used, as they allow a systematic control of the tested parameters and lead to simple expressions for the roughness factor.

An exhaustive review on various of these criteria was presented by Moita and Moreira [24] from which, for the regular pattern considered in the present work (square cavities/pillars) the most accurate criteria to differentiate homogeneous vs heterogeneous wetting is given as in Figure 3, which results from the analysis of the work of Jung and Bhushan [25]. Here, the governing geometric parameter is the ratio h_R/S, where h_R is the size of the pillars/cavities and S is the distance between them.
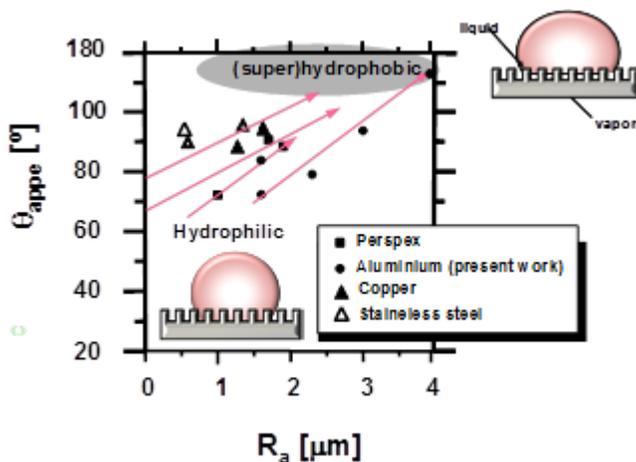
For the superhydrophobic surfaces, stable heterogeneous wetting regimes require hierarchical roughness patterns (e.g. Gao et al. [26]), which often render a stochastic profile, that is more difficult to analyse. In this case, the use of the apparent contact angle to set a wetting trend must be done with care. For instance, as they are defined, the Wenzel and the Cassie and Baxter equations state roughening a hydrophilic surface will make it more hydrophilic and roughening a hydrophobic surface will turn it to be more hydrophobic. That is true in the extreme situations, but different trends may actually occur within the same wetting regime, as several variations on the roughness profile may not be exactly well captured by the macroscopic apparent angle. In the case of the stochastic profiles, the problem is more complex, as the roughness must be quantified by average quantities, which do not account for the detailed geometric properties associated to the size, depth and shape of the surface asperities. Additional statistic treatment may provide interesting information, (e.g. Hitchcock et al. [27]), but still will not capture the topology of the surface. Similarly to the parameter h_R/S, proposed for regularly patterned surfaces, Hitchcock et al. [27] suggest to relate the apparent equilibrium angle with the surface roughness quantified as R_a/λ, being R_a the mean roughness and λ the fundamental wavelength, which was estimated based on the FFT analysis of the profiles. In most situations, λ was found to be related to periodical waviness of the surfaces caused by their manufacturing process and therefore in most of the cases a relation between the apparent equilibrium angle and the mean surface roughness R_a was adopted.

In line with this, Figure 4 depicts the apparent equilibrium angle as a function of R_a for various surfaces and materials, including those used in the present work (stochastic profiles). The contact angles are measured for water at room temperature

(20ºC). The values are quite scattered due to the influence of the chemistry of the surface (surface composition), but looking at measurements obtained for the same surface material, the trend of the surface to become more hydrophilic with increasing roughness amplitude is not so clear. Actually, within the homogeneous wetting regime (i.e. following Wenzel equation), in which the surfaces are essentially hydrophilic the results suggest an increase of the contact angle with R_a. This trend is in agreement with the results reported by Hitchcock et al. [27], for a similar range of R_a and is opposite to the findings of Kandlikar and Steinke [28], although the later considered smoother surfaces.

Figure 3 Definition of the wetting regimes for regular patterned surfaces with square pillars/cavities.

Figure 4 Definition of the wetting regimes for surfaces with stochastic roughness profiles.

The main issue to consider here is, once again, the scale of measure of the contact angle and how it is being affected by the scale of the surface topography. Even at the macroscopic scale, different roughness amplitudes are enough to produce contrasting results (e.g. between [27] and [28]).

So, overall, the Wenzel and Cassie and Baxter equations are useful to estimate the wetting regime, but mild effects (for instance of surface topography) may not be captured by the apparent angle. Hence, the actual wetting regime should be checked based on the visualization of the contact line. In the present work, the liquid-solid interface was verified with optical microscopy. Further accuracy is however desired, for instance with confocal microscopy.
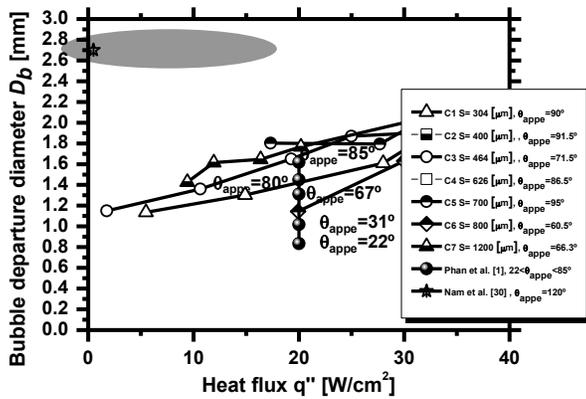
The wettability is known to deeply affect the basic nucleation processes, which consequently will influence the pool boiling heat transfer. The following paragraphs will discuss the potential use of the apparent contact angles (static and dynamic) to describe the nucleation process.

Quantification of the role of wettability on nucleation and bubble dynamics
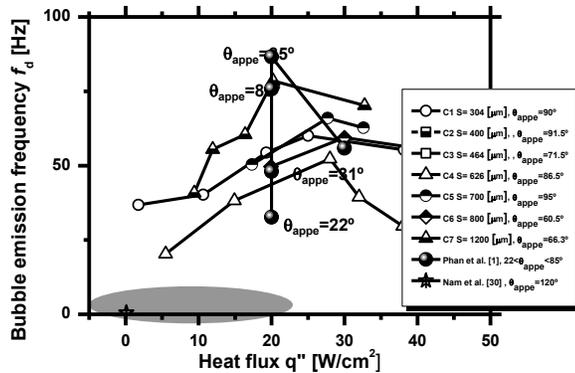
The role of surface wettability is determinant in the mechanisms of bubble formation and departure. The balance between buoyancy and interfacial forces governs the bubble growth and departure, although a non negligible effect of the shear lift force and of the quasi-static drag force is argued by a few authors (e.g. Matkovic and Konkar [29]). However, [29] conclude that the main uncertainty in theoretical determination of the departure diameter was related to the value of the contact angle and to the determination of the component of the surface tension force. This was particularly noticeable for superhydrofobic surfaces.

Taking, as for most of the reported studies, the apparent contact angle as the quantity to be directly related to the bubble departure mechanism, one may analyse the trend of the bubble departure diameters and emission frequencies for water pool boiling on hydrophilic and superhydrophobic surfaces, as shown in Figures 5 and 6, respectively. The experimental data of Phan et al. [1] is gathered here for comparative purposes.

The results shown here are limited to relatively low heat fluxes (q"<40Wcm^{-2}), given that for the hydrophobic surfaces, the onset of boiling occurs for very low heat fluxes and just 1-3ºK of surface superheat, so the values obtained for these surfaces would be very difficult to read when compared with the results obtained for the hydrophilic surfaces. Also, very little data is available up to know under these conditions for the superhydrophobic surfaces because the coalescence occurs already at these very low heat fluxes and surface superheat values. All the other fluids are not shown here because all the surfaces became lyophilic with them. The results depicted in Figures 5-6 should be analysed globally, as a function of the apparent contact angle. By doing so, two significantly different trends can be identified, once again within the two opposite regimes hydrophilicity/superhydrophobicity: the bubbles observed in the boiling of water on the superhydrophobic surface are significantly larger than those obtained for any of the hydrophilic surfaces. Although the experimental evidence does not totally validate it yet, most of the relations in the literature determine an inverse proportionality between the bubble departure diameter and the emission frequency. Overall, this is an existing trend, so it is understandable that the emission frequency of the bubbles over the superydrophobic surfaces are about 100times lower than those observed over the hydrophilic ones. This is in agreement with the results reported by Nam et al. [30].

Figure 5 Bubble departure diameter water boiling over hydrophilic and superhydrophobic surfaces identified with the apparent equilibrium angle.
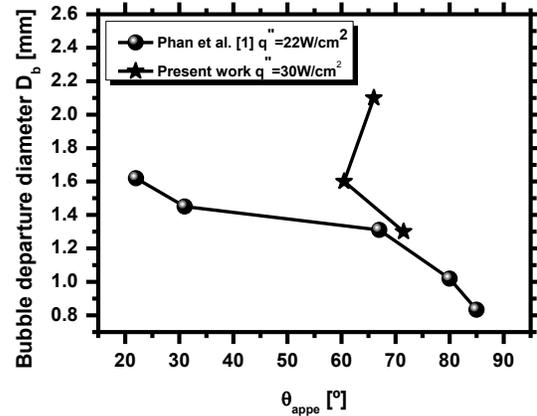

Figure 6 Bubble emission frequency water boiling over hydrophilic and superhydrophobic surfaces identified with the apparent equilibrium angle.

Hence, the trend from hydrophilic to superhydrophobic surfaces is that the bubble departure diameter increases with the apparent contact angle, which is in agreement with most of the correlations predicting this quantity, as they usually derive from the Fritz equation [31]:

$$D_b = f(Lc, \theta_{appe}) \qquad (5)$$

where Lc is the characteristic capillary length, which is representative of the size of the bubble $Lc = (\sigma_{lv}/g(\rho_l - \rho_v))^{1/2}$, being σ_{lv} the interfacial liquid-vapor surface tension, g the acceleration of gravity and ρ_l and ρ_v the liquid and vapor densities. However, looking at the local trends inside the evolution from hydrophobic to hydrophilic surfaces, the aforementioned relation between the apparent equilibrium angle and the bubble diameter is not so clear. Focusing now on the evolution of the departure diameter, as a function of the apparent equilibrium angle, for constant values of the heat flux, as represented in Figure 7, the results suggest that within the hydrophilic regime, the departure diameter actually tends to decrease as the apparent contact angle increases up to 90º. In the present study that trend is not so clear as in Phan et al [1] because the bubble diameters are also being affected by interaction mechanisms cause by the surface roughness, which

are not captured by the apparent angle. However, overall, the trend of Phan et al. [1] is observed.

Figure 7 Bubble departure diameter as a function of the apparent contact angle, within the hydrophilic regime, i.e. while $\theta_{appe} < 90º$.

At lower heat fluxes, for which a wider range of apparent contact angle values can be analysed, due to the chemical modification of the surface (results of Phan et al. [1]), this trend is quite clear. For higher heat fluxes, where mainly the surfaces obtained (in the present study) are hydrophobic, or hydrophilic with relatively high apparent contact angles, the values of the diameter are more scattered as a function of the apparent angle. This is due to the fact that, in this case, surface topography modifications are not scaled to affect the apparent angle, but are still influencing the bubble mechanisms near the surface (namely the interaction mechanisms). To account for these effects, previous work considered the use of the so-called coalescence factor and a roughness parameter relating the characteristic size of the bubbles with the distance between the micro-cavities S/Lc. (e.g. [32]).

Phan et al [33] provide a feasible explanation for the contrasting trends reported in their previous work (Phan et al. [1]) which are also evident here, when gathered with the results obtained in the present work: the micro-scale contact angle at bubble formation is within a microscopic scale and therefore different from that of the apparent angle. In fact, at boiling conditions, the balance between the interfacial forces becomes unstable due to the heat flux imposed at the interface of the bubble, which promotes evaporation near the contact line. Under these conditions, the curvature of the contact line changes. So, the hydrophilic nature of the surface is actually defined by the intensity and direction of the surface tension force applied to the contact line, which for the hydrophilic surfaces will contribute to maintain the bubble attached to the surface. As the micro-contact angle defined at the bubble increases, the vertical component gets towards the surface and the bubble detaches. So the bubbles actually grow bigger and stay attached to the surface for longer, as this micro-scale angle is smaller. Hence, the micro-scale contact angle controls the vertical component of the surface tension during the process of the bubble growth and only afterwards tends, according to Phan et al. [33] to get closer the apparent angle. Following this last

approximation of the micro to the apparent contact angle, at the end of their work, Phan et al. [33] simply adjust the correlation between the bubble departure diameter and the apparent contact angle to capture the new trend (i.e. for hydrophilic conditions the bubble diameter actually decreases with the apparent contact angle), and considered that the bubble diameter, made dimensional with the characteristic length Lc is proportional to tan $\theta_{appe}^{-1/6}$. Generally, as these authors recognize, this kind of correlations capture well the global trends of the size of the bubbles and are not much sensitive to the variation of the apparent contact angles. However, they lack important information that is not gathered in the apparent contact angle. Deeper work is required to validate this theory, but the discussion made up to now can be important for the superhydrophobic cases as well, for which the relation with a stochastic profiles and the apparent contact angle can be even more difficult to capture with the apparent contact angles (as shown in Figure 3). Also, in the present study, there is an interaction and coalescence effect caused by the surface topography that is naturally more likely to occur for the superhydrophobic surfaces and which is, once again, not captured by the apparent angle.

Taking the concept of the micro-scale contact angle and considering that the nature of the superhydrophobic surface is again related to the surface tension forces directly acting on the moving contact line, in this case the evaporative effect leads the bubble to stay attached to the surface. Now, as the contact line moves, there is any component of the surface tension contributing for the bubble to detach from the surface. Consequently, the bubble stays growing for longer, as shown quantitatively in Figure 5, so the growing bubbles re more likely to coalesce. This is in line with various observations reported in the literature (e.g. [30]). The coalescence will further delay the bubble emission frequency.

Hence, bubble departure diameter is proposed to be:

$D_b = f(Lc, \theta_{ms}, S/Lc)$ (6)

The roughness geometrical parameter S/Lc is eventually required as it represents the effect of the surface topography (e.g. on the interaction mechanisms), that is not captured by the micro-scale contact angle, but that is not being well captured by the apparent contact angle either.

In summary, the micro-scale contact angle assures to capture the actual balance of the forces which are actually acting at the contact line, during the bubble growth and detachment. The apparent contact angle is nevertheless useful to identify the wetting regimes and describe global trends in opposite scenarios. It is worth studying in detail the evolution of the micro-scale contact angle to determine the exact conditions for which it is approximated to the apparent angle, as argued by Phan et al. [33]. The problem may be partially solved by using advancing and receding contact angles, as suggested by Mukherjee and Kandlikar [34] 2007. However, the most accurate measurements of the contact angle are not obtained under dynamic conditions, but instead for quasi-static angles, which are still not representative of the motion of the contact line. It is worth noting that our results do not sustain that the macroscopic apparent angle is approximated to the micro-scale angle. Any clear trend can be observed between the

apparent angle and the bubble dynamics, as the latter is being influenced by surface topography in a way that is clearly not captured by the apparent angle. Hence, a deeper study is required to define the exact conditions for which the macro and the micro-scale angles can be related.

The bubble dynamic processes will naturally affect the heat transfer process, so that heat transfer coefficients should also address the aforementioned proposed relation for the bubble departure diameters.
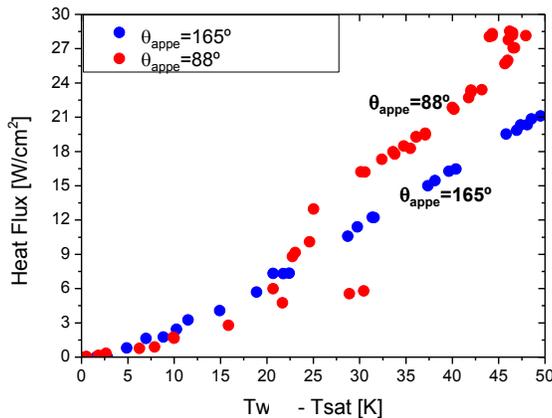
Multi-scale approach to describe pool boiling heat transfer

The discussion performed so far stands for the argument that the apparent equilibrium angle is useful to identify general trends in opposite wetting scenarios, but it must be related to the micro-scale angle, which in turn determines the bubble dynamic process. The heat transfer occurring at pool boiling is naturally dependent on the bubble dynamics so that a similar argument should sustain here. Figure 8 depicts the boiling curves obtained for two extreme wetting scenarios, namely water pool boiling over a hydrophilic and a superhydrophobic surface, identified by the apparent equilibrium angles. Consistently with the bubble dynamics process, discussed in the previous paragraphs, the onset of boiling occurs at very low values of the heat flux and of surface superheat (up to 5K), so that up to superheat values of 20K, for the same superheat value, the heat flux for pool boiling over the superhydrophobic surface is higher.
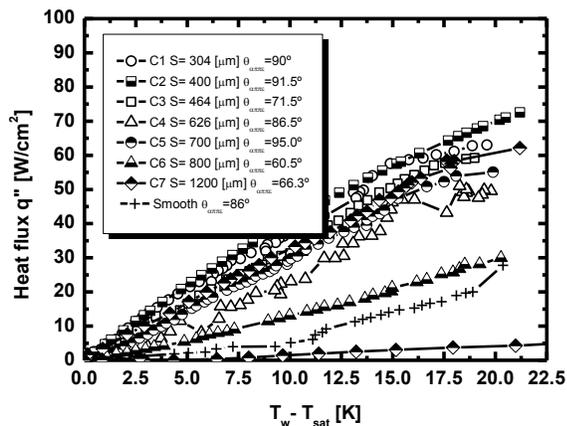
This trend is ultimately inverted since the big bubbles formed over the superhydrophobic surface start to coalesce, also at very low values of the surface superheat, thus leading to a Critical Heat Flux scenario for much lower superheat values, when compared to the hydrophilic surface. The apparent angle can be used to differentiate the curves obtained in extreme wetting scenarios, but once again, looking closer within the contact angle ranging from hydrophilic to hydrophobic (close to 90º), it is not possible to identify any trend between the apparent angle and the evolution of the boiling curves, since they are being affected, as already explained in Moita et al. [35] and in Teodori et al. [36] by topographical parameters (S/Lc), which however, are not scaled to affect the apparent contact angle (Figure 9). These results can be also explained based on a micro-scale analysis, as proposed by Phan et al. [1] and clearly described by Moreira [6]: high heat transfer occurs at the contact line, which is theoretically aided by a liquid microlayer. Inside the bubble, adhesive forces preclude heat transfer and outside, the thermal resistance of the bulk liquid region also prevents the heat transfer. The early high heat transfer at the contact line promotes the change in shape and favours the evolution of the micro-scale contact angle that was discussed for the bubble growth for the hydrophilic vs hydrophobic cases, respectively. The opposite trend occurs for the superhydrophobic surface, which, as the bubbles stay attached to the surface and start to coalesce, will make the heat transfer more difficult and preclude the liquid circulation over the surface.

Within the hydrophilic surfaces, the different boiling curves are mainly due to coalescence effects, which are not caused by the shape of the bubbles (role of the wettability, described by

the micro-scale angle), but by the surface topography, as a too small distance between cavities will also promote coalescence [32-36].

Figure 8   Boiling curve of water over a hydrophilic and a superhydrophobic surface.

Figure 9   Boiling curve of water over a hydrophilic micro-structured surfaces. Here there is no evident trend between the boiling curve and the apparent contact angle.

FINAL REMARKS

The present paper discusses the quantity that should be used to accurately describe the role of wettability on pool boiling heat transfer. The most commonly used parameter to quantify the wettability is the apparent contact angle, but this is a macroscopic quantity that is used to describe micro and nano scale phenomena that occur at the contact line.

Analyzing the wetting behaviour of numerous surfaces, based on the apparent contact angle, it is evident that this angle is useful to estimate the wetting behaviour a priori, but cannot capture several microscopic effects (for instance of surface topography). Quasi-static and dynamic contact angles can provide additional information, but still only within a macroscopic scale.

In line with this, apparent contact angles can be used to establish general trends and differentiate bubble dynamics behaviour occurring for opposite wetting regimes. However,

milder wetting changes occurring within each regime, caused, for instance, by surface topography are not well captured by the apparent angle, as the surface topography is not scaled to affect this macroscopic angle, although it can clearly influence the bubble formation and departure mechanisms and, consequently the heat transfer coefficients. The apparent angle is not approximated to the microscopic one and a deeper study is required to understand the relation between them. Introducing the concept of the micro-scale contact angle, as proposed by Phan et al. [1], together with a geometrical parameter to include the effect of surface topography, allows describing the role of the wettability on bubble dynamics. Based on this analysis, a multi-scale approach is proposed to include the role of wettability on correlations predicting the pool boiling heat transfer coefficients.

ACKNOWLEDGEMENTS

REFERENCES

[1] Phan, H.T., Caney, N., Marty, P., Colasson, S. and Gavillet, J., Surface wettability control by nanocoating: the effects on pool boiling heat transfer and nucleation mechanism, *Int. J. Heat Mass Transf.,* vol. 53, 2009, pp. 5459-5471.

[2] Corty, C. and Foust, A.S., Surface variables in nucleate boiling, *Chem. Eng. Prog. Symp. Ser.,* vol. 57, No. 17, 1955, pp. 1-12.

[3] Takata, Y., Hidaka, S., Uraguchi, T. and Hu, L.W., Boiling feature on a super water-repellent surface, *Heat Transf. Eng.*, vol. 27, 2006, pp. 25-30.

[4] Nam, Y. and Ju, Y.S., Bubble nucleation on hydrophobic islands provides evidence of anomalously high contact angles of nanobubbles, *Appl. Phys. Lett.,* vol. 93, 2008, pp. 103115.

[5] Cheng, P., Quan, X.J., Gong, S. and Hong, F.J., Recent studies on surface roughness and wettability effects in pool boiling, *Proc. IHTC-15, Kyoto, Japan, August 2014.*

[6] Moreira, A.L.N., Multi-scale interfacial phenomena and heat transfer enhancement, *Proc. IHTC-15, Kyoto, Japan, August 2014.*

[7] Gambaryan-Roisman, T., Controlling hydrodynamics, heat transfer and phase change in thin films and drops, *Proc. IIHTC-15, Kyoto, Japan, August 2014.*

[8] Young, T., An essay on the cohesion of fluids, *Phil. Trans. R. Soc. Lond.*, vol. 95, 1805, pp. 65-87.

[9] Wenzel, R.N., Resistance of solid surfaces to wetting by water, *Ind. Chem. Eng. Chem.*, vol. 28, 1936, pp. 988-994.

[10] Cassie, A.B. and Baxter, S., Wettability of porous surfaces, *Trans. Faraday Soc.*, vol. 40, 1944, pp. 546-551.

[11] Marmur, A., Measures of wettability of solid surfaces. *The European Physical J. Special Topics*, vol. 197, No. 1, 2011, pp. 193–198.

[12] Gao, L. and McCarthy, T.J., How Wenzel and Cassie were wrong, *Langmuir*, vol. 23, No., 7, 2007, pp. 3762-3765.

[13] He, B., Patankar, A. and Lee, J., Multiple equilibrium droplet shapes and design criterions for rough hydrophobic surfaces, *Langmuir,* vol. 19, 2003, pp. 4999-5003.

[14] Betz, A.R., Jenkins, J., Kim, C.-J- and Attinger, D., Boiling heat transfer on superhydrophilic, superhydrophobic and biphilic surfaces, *Int. J. Heat Mass Transf.*, vol. 57, 2013, pp. 733-741.

[15] Hsu, C.-C. and Chen, Surface wettability effects on critical heat flux of boiling heat transfer using nanoparticle coatings, *Int. J. Heat Mass Transf.*, vol. 55, 20012, pp. 3713-3719.

[16] Bourdon, B., Rioboo, R., Marengo, M., Gosselin, E. and De Coninck, J., Influence of the wettability on the boiling onset, *Langmuir*, vol. 28, 2012, pp. 1618-1624.

[17] Bourdon, B., Di Marco, P, Marengo, and De Coninck, J., Enhancing the onset of pool boiling by wettability modification on nanometrically smooth surfaces, *Int. Comm. Heat Mass Transf.*, vol. 45, 2013, pp. 11-15.

[18] Moita, A.S. and Moreira, A.L.N., Scaling the effects of surface topography in the secondary atomization resulting from droplet/wall interactions, *Exp. Fluids*, vol. 52, No. 3, 2012, pp. 679-695.

[19] Pereira, P. M. M., Moita, A.S., Monteiro, G. A. And Prazeres, D.M.F., Characterization of the topography and wettability of English weed leaves and biomimetic replicas, *J. Bionic Eng.*, vol. 11, 2014, pp. 346-359.

[20] Cheng, P., Automation of axisymmetric drop shape analysis using digital image processing., *PhD Thesis*, University of Toronto, 1990.

[21] Bushan, B. and Jung, Y.C., Natural and biomimetic artificial surfaces for hydrophobicity, self-cleaning, low adhesion and drag reduction, *Prog. Mat. Sci.*, vol. 56, 2011, pp. 100-108.

[22] Abernethy, R.B., Benedict, R.P. and Dowdell, R.B., ASME measurement uncertainty, *J. Fluids. Eng.*, vol. 107, No. 2, 1985, pp. 161-164.

[23] Moita, A.S., Teodori, E. and Moreira, A.L.N., Effect of surface topography in the boiling mechanisms, *Int. J. Heat Fluid Flow*, vol. 52, 2015, pp. 50-63.

[24] Moita, A. S. and Moreira, A. L. N., From single droplet impact to micrometric droplet chains: scaling the effect of surface topography. *Proc. 12th International Conference on Liquid Atomization and Spray Systems - ICLASS 2012,* Heidelberg, Germany, September 2012.

[25] Jung, Y.C. and Bhushan, B., Dynamic effects of bouncing water droplets on superhydrophobic surfaces, *Langmuir*, vol. 24, 2008, pp. 6262-6269.

[26]Gao, N., Yan, Y., Chen, X. and Mee, D.J., Superhydrophobic surfaces with hierarchical structure, *Mat. Lett.*, vol. 65, No. 19-20, 2011, pp. 2902-2905.

[27] Hitchcock, S.J., Carrol, N.T. and Nicholas, M.G., Some effects of surface roughness on wettability, *J. Mat. Sci.*, vol. 16, 1981, pp. 714-732.

[28]Kandlikar, S.G. and Steinke, M.E., Contact angles of droplets during spread and recoil after imping on a heated surface., J. Ch. Eng. Res. Des., vol 79, 2001.

[29] Matkovic, M. and Koncar, B., Bubble departure diameter prediction uncertainty, *Sci. Tech. Nuclear Ind. Inst.*, vol. 2012, ID 863190, 7p.

[30] Nam, Y., Wu, J. and Ju, Y.S., Experimental and numerical study of single bubble dynamic on a hydrophobic surface, *ASME J. Heat Transf.*, vol. 131, 2009, pp. 121004-1-121004-7.

[31] Fritz, W., Maximum volume of vapor bubbles, *Phys. Z*, vol. 36, 1935, pp. 279-385.

[32] Moita, A. S., Teodori, E. and Moreira, A.L.N., Enhancement of pool boiling heat transfer by surface micro-structuring, *J. Phys.: Conf. Series*, vol. 395, 2012, pp. 012175.

[33] Phan, H.T., Bertossi, R., Caney, N., Marty, P. and Colasson, S., A model to predict the effect of surface wettability on criticall heat flux, *Int. Comm. Heat Mass Transf.*, vol. 39, 2012, pp. 1500-1504.

[34] Mukherjee, A. and Kandlikar, S.G., Numerical study of single bubbles with dynamic contact angle during nucleation pool boiling, *Int. J. Heat Mass Transf.*, vol. 50, 2007, pp. 127-138.

[35] Teodori, E., Moita, A.S. and Moreira, A.L.N., Characterization of pool boiling mechanisms over micro-patterned surfaces using PIV. *Int. J. Heat Mass Trans.*, vol. 66, 2013, pp. 261-270.

[36] Teodori, E., Moita, A.S. and Moreira A.L.N., Empirical correlations between bubble dynamics and heat transfer coefficient for pool boiling over micro-textured surfaces. *Proc. 17th Int. Symp. Laser Techniques Applied to Fluid Mechanics*, Lisbon, Portugal, July 2014.